Experimental investigation of a new turbocharged concentrating solar air heater

Antonio Famiglietti[1,2], Antonio Lecuona-Neumann[1] and Javier Roa[2]

1 Universidad Carlos III de Madrid, Departamento de Ingeniería Térmica y de Fluidos, Avda. de la Universidad 30, 28911 Leganés, (Spain)

2 Demede Engineering and Research, Laguna de Marquesado 47, 28021, Madrid (Spain)

Abstract

Although still uncommon, direct air heating inside a linear concentrating collector can be a suitable solution for industrial hot air production aiming at environmental sustainability and decarbonization. In order to demonstrate the technical feasibility and investigating the key features of the technology, an experimental prototype is installed and tested. A small-scale solar field with 79.2 m^2 of linear Fresnel collectors is coupled with an automotive turbocharger to reduce the pumping power in an innovative layout. A compressor increases air pressure before it is heated up to 450 - 500 °C inside evacuated receivers. The turbine recovers the compressing power. Hot air at 300 - 400 °C is provided at the turbine exit, available for usage. Results enable the characterization of the main components and system behavior, establishing critical design and operational aspects.

Solar air heater; linear Fresnel collector; Solar heat for industrial processes; Industrial drying

1. Introduction

The use of air as heat, moisture and other vapor carrying fluid is widespread in the industry. Drying and thermal curing are high energy demanding processes requiring hot air, which is common to several industrial sectors, including agricultural, food and beverage, pharmaceutical, mining, wastewater and residues treatment, manufacturing, among others. Process hot air at low and medium temperatures is currently provided from fossil fuel combustion as well as from electricity, which has only a partial renewable energy share. Solar thermal energy has great potential as an alternative source, aiming at decreased pollution and decarbonization. Air solar collectors can heat ambient air up to ~100 ℃ without the need for a primary heat transfer fluid HTF. For applications requiring higher temperatures, linear concentrating collectors are a suitable alternative to conventional air heating systems. Both linear Fresnel collector LFC and parabolic trough collector PTC have been considered for industrial indirect hot air production above 150 °C, as reported by (Farjana *et al.*, 2018) and (SHIP Database). Some experimental research was performed by (Zahler and Iglauer, 2012) and (Rehman *et al.*, 2019). These solutions require a proper primary HTF, such as thermal oil or pressurized water, for heat evacuation from the collector receiver and downstream delivery to process air through an HTF/air heat exchanger HX.

Direct solar air heating in concentrating collectors would avoid the use of HTFs and HXs and their related costs, risk of spillage, and maintenance, although, their use is still uncommon. (Famiglietti *et al.*, 2020) indicates that the main drawback of direct solar air heating in concentrating collectors using conventional evacuated receivers is the high pumping power requirement, due to low thermal diffusivity and high kinematic viscosity, besides the overheating risk of receiver tube due to low internal heat transfer rate. They proposed an innovative turbo-assisted solar air heater T-SAH, involving an automotive turbocharger to mitigate these drawbacks. The compressor increases the air density in the receiver, reducing flow velocity and stagnation pressure drops. Meanwhile a turbine provides compressing and pumping power, avoiding the external auxiliary energy consumption. This enables higher air mass flow rate, thus preventing the receiver overheating risk. These authors demonstrate that hot air up to 300 – 400 °C can be provided at the turbine outlet. The concept of turbo-assisted solar air heater T-SAH is further investigated numerically by (Famiglietti *et al.*, 2021) simulating a medium-scale solar field of linear Fresnel collectors coupled with a commercial automotive turbocharger. The present work summarizes the main experimental results obtained from an original prototype of the T-SAH described in Section 2, using a 79.2 m^2 of linear Fresnel collectors and a small off-the-shelf turbocharger.

doi:10.18086/swc.2021.22.02 Available at http://proceedings.ises.org

2. Experimental setup

The prototype of a turbocharged concentrating solar air heater was installed on the rooftop of Carlos III University of Madrid (Spain), in the city of Leganés. Fig.1 shows its layout.

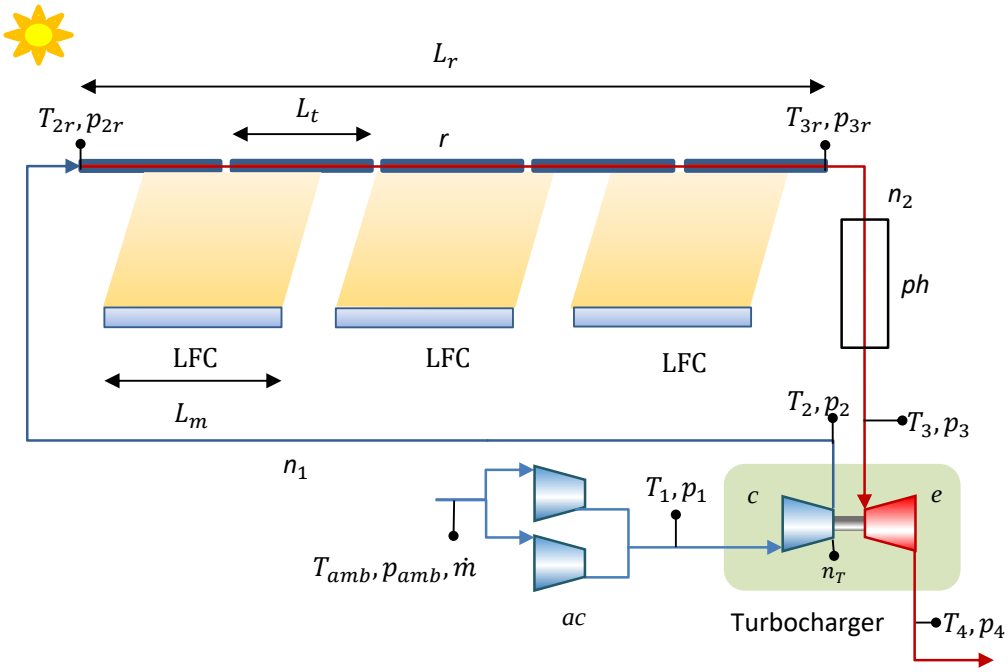

Fig.1: Experimental setup of T-SAH installed at Carlos III University of Madrid, Linear Fresnel Collector LFC, auxiliary compressor ac, turbo-compressor c, turbine e, post-heating unit ph.

The solar field consists of three linear Fresnel collectors LFCs installed in series, equipped with five standard evacuated tubes. The LFC is the first generation of a commercial module developed and manufactured by (Solatom™). The primary reflector is composed by 10 curved mirrors of $w_m = 0.50$ m aperture, rotated around horizontal axis with individual tracking motors. The secondary reflector has trapezoidal shape and aims to recover the concentrated irradiance missing the receiver. An original feature of the collector is foldability. The primary reflector structure is made of two foldable wings. In addition, the secondary receiver includes a mechanism for sliding it up and down. When folded and closed, the collector is containerized into a rectangular-shaped box and can be easily transported. The module is pre-assembled in the factory and transported to the installation place already calibrated and tuned. Fig. 2(a) shows a downstream view the solar field tracking the sun.

The receiver is of the single tube type and consists of standard evacuated tubes manufactured by (Archimede Solar Energy™), originally developed for thermal oil HTF (model HCEOI-12). The stainless-steel tube having external diameter of $D_{ex} = 70$ mm is covered by selective coating and embed into a concentric vacuum glass tube of high transparency. The selective coating has a maximum operating temperature of 580 °C and a maximum allowable temperature of 600 °C.

(a) (b)

Fig. 2. Experimental installation at Carlos III University of Madrid, Leganés (Spain). (a) Downstream view of the solar field on tracking, primary and secondary reflector, and receiver tubes, (b) turbocharger (before thermal insulation).

The required air temperatures inside the receiver induce high receiver temperatures and a consequent non-negligible axial thermal dilatation. Considering the thermal linear expansion coefficient of stainless steel of $0.016 \frac{\text{mm}}{\text{m K}}$, dilatation over the total tube length $L_t = 20$ m is estimated between 100 mm and 200 mm. Accordingly, receiver tubes have been provided with sliding support brackets, avoiding mechanical stress and compression buckling, Fig.2. The dilatation of the receiver with respect to the glass cover evacuated tube is compensated by bellows according to the receiver manufacturer's design.

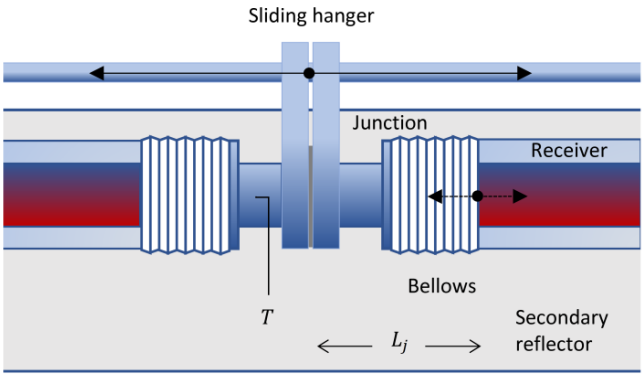

Fig.3. Schematic of sliding junction between consecutive receiver tubes

An automotive journal bearings turbocharger (GT1544 (Garrett Advancing Motion)) has been connected to the receiver through thermally insulated piping, Fig.2(b). The compressor wheel has a diameter of $D_c = 43.9$ mm, with a TRIM (the ratio between smallest and highest wheel area) of 56%. The turbine has a wheel diameter is $D_e = 41$ mm and TRIM of 58%.Two parallel electrical blowers (Elektor SD22 FU 80/1,1) are installed in series with the turbocompressor, controlled by a variable frequency converter (Lense 8200 vector) as an auxiliary source of power.

An auxiliary post-heating unit has been provided for additional experimentation. They were mounted downstream of the solar collectors to further increase the inlet turbine temperature according to the

experimental tests devised. It is made of electrical resistances with a limiting temperature of 650 - 700°C able to generate 8 kW of thermal power.
The set-up is instrumented by placing Type K thermocouples class A and pressure sensors in several points of the air circuit, according to Fig.1, with an estimated uncertainty of ± 2.0 °C and ± 25 mbar respectively. Airflow is measured at the inlet using a sensor having an uncertainty of ±3% (Schmidt 30.015 MPM). Rotational turbocharger speed is measured by an optical speed sensor with +/-0.05% uncertainty. Two pyranometers (Kipp & Zonen) with ±3% total uncertainty measure global solar irradiance G_{glo} on the horizontal plane and diffuse irradiance G_d. Monitoring and data acquisition with a time interval of 30 s was enabled by a dedicated SCADA, implemented in a Programmable Logic Controller PLC (Unitronic USP-104-B10). Tab.1 reports relevant prototype parameters.

Table 1. Prototype parameters.

LFC active length	L_m	5.28 m	Overall receiver length	L_r	20.65 m
LFC aperture width	W_a	5.00 m	Receiver internal diameter	D	0.066 m
Height receiver	H_m	2.72 m	Overall active area	$n_s A_m$	79.2 m^2
LFC active area	A_m	26.40 m^2	Connection pipe 1	L_{n1}	26 m
Normal optical efficiency	η_{op0}	0.632	Connection pipe 2	L_{n2}	3 m
Mirrors per module	n_m	10	Connection internal diam.	D_n	0.08m
Mirror aperture width	w_m	0.50 m	Orientation (0 = South)	γ_r	54.3 deg W
LFC in series	n_s	3	Latitude	Φ_{loc}	40.165 deg N
Max. temperature receiver	$T_{w,max}$	600°C	Longitude	λ_{loc}	3.704 deg W

3. Results

Several tests have been carried out on the T-SAH prototype, described in Section 2 aiming at the full characterization of the innovative T-SAH concept. The first one was conducted by running the prototype across a summer day with a clear sky. Solar air heating was performed in the best conditions to reach maximum solar power and air temperature at the receiver outlet, without the post-heating power aid. This allows studying the global behavior of the system, including the solar field, the turbocharger, and the auxiliary compressor. A second representative test, also performed during summer and clear sky conditions, was devised for the turbocharger characterization. The additional thermal power delivered by the post-heater allows increasing the turbocharger testing range, due to higher inlet turbine temperature. This way, additional solar aperture area can be simulated.

Fig. 4 reports the experimental results obtained during the first representative test. During the clear summer day, the turbocharger is accelerated through the auxiliary electrical blowers and three solar collectors are in sun-tracking mode. The post-heating unit is OFF. A thermal transient is established during the first hour of operation, due to piping and receiver tube thermal inertia. Then, quasi-steady-state conditions are achieved, with the turbocharger speed varying slightly with outlet receiver temperature. Fig.4(a) shows the main temperatures across the True Solar Time TST. The peak air temperature at the receiver outlet $T_{3r} > 500$ °C is reached at solar midday. At the compressor outlet air holds a temperature $80\ °C < T_2 < 130\ °C$, according to the increased pressure. Air is delivered at the turbine outlet at $300\ °C < T_4 <$400 °C. The pressure inside the receiver tubes, which is imposed by the turbocharger varies across the TST up to 1.4 bar, as shown in Fig.4(b). Air mass flow rate $\dot{m}_a$ also varies according to turbocharger speed, Fig. 4(c). Fig. 4(d) depicts the main power contributions. Solar power delivered to airflow in the receiver reaches 17 kW at solar midday $\dot{Q}_u$, while the thermal power at the outlet air flow $\dot{Q}_a$ is affected by the thermal losses in the sending and return piping $\dot{Q}_{n1}$ and $\dot{Q}_{n2}$.
The over-pressure imposed by the auxiliary blower decreases as turbocharger speed increases, Fig. 4(b).

$$\dot{Q}_u = (T_{3r} c_{p3r} - T_{2r} c_{p2r})\, \dot{m}_a \quad \text{(eq.1)}$$

$$\dot{Q}_a = (T_4 c_{p4} - T_{amb} c_{pamb})\, \dot{m}_a \quad \text{(eq.2)}$$

$$\dot{Q}_{n1} = (T_2 c_{p2} - T_{2r} c_{p2r})\, \dot{m}_a \quad \text{(eq.3)}$$

$$\dot{Q}_{n2} = (T_{3r} c_{p3r} - T_3 c_{p3})\, \dot{m}_a \quad \text{(eq.4)}$$

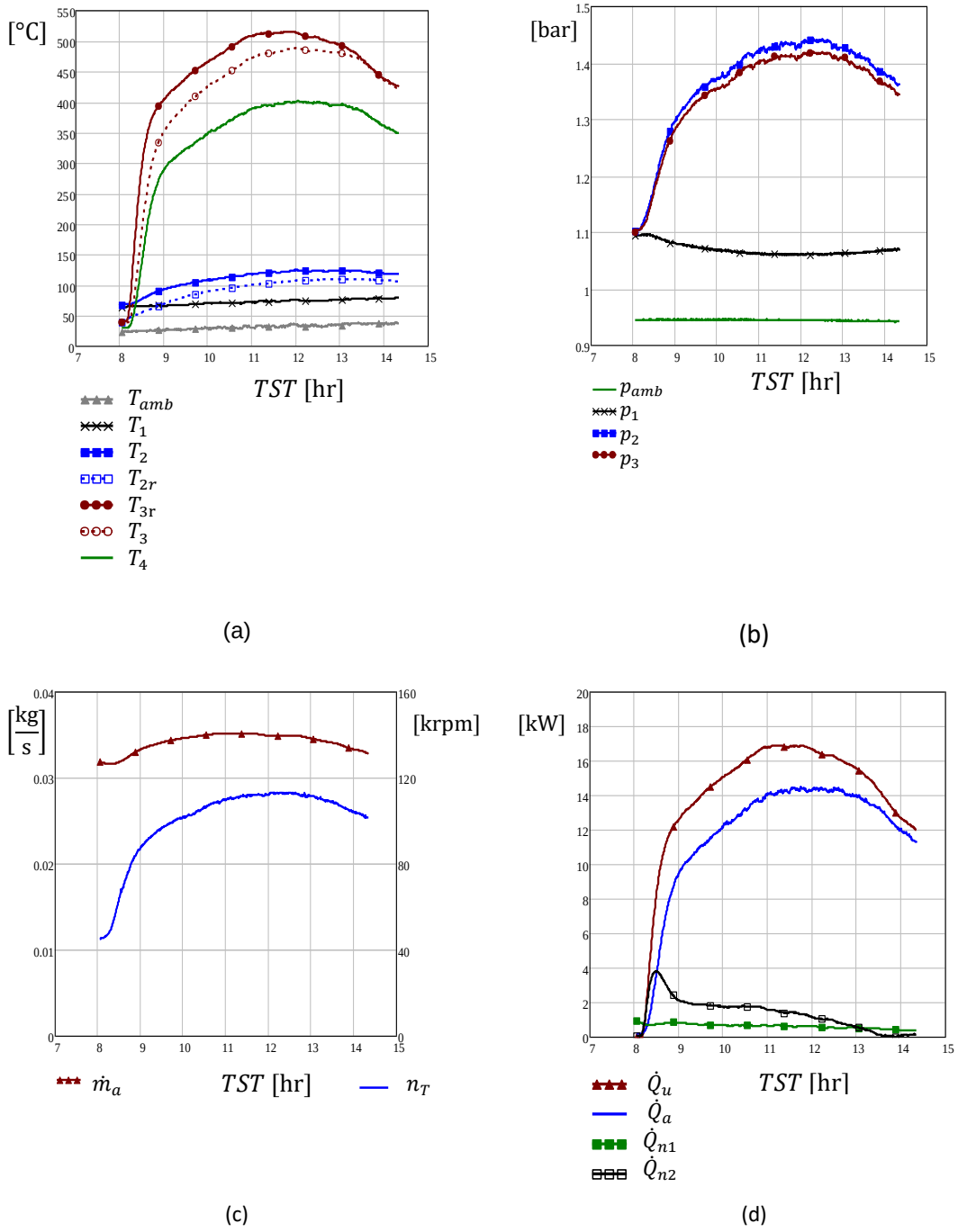

Fig.4. Experimental results, T-SAH operation along a sunny summer day, experimental post-heating OFF, vs. true solar time. (a) Temperatures. (b) Pressures. (c) Mass flow rate and rotating speed. (d) Thermal powers.

The experiment demonstrates the feasibility of direct air heating inside a linear Fresnel collector at moderate pressure, not previously documented in the open literature. Due to the low heat capacity of air, 500 °C of temperature can be reached even in small collector rows as the present one. According to the technical literature, excessive receiver tube bending is recognized as a risk of glass cover breakage, when the tube lateral displacement makes it touch the cover glass tube. This is effect is expected to be a relevant issue when the evacuated tube operated with low internal heat transfer, typical of gaseous flows and with non-uniform circumferential heat flux distribution, which results from the optical concentration either in LFCs and PTCs. In the present experiment, bending has been observed, especially during the starting transient when tubes still encompass circumferential temperature homogenization. Nevertheless, no damage to the cover glass occurred. Secondary reflector with trapezoidal as in the present setup, or more performing ones as compound parabolic

optics, seems beneficial for distributing the solar heat flux across the receiver perimeter, reducing the tube bending.

The direct air heating using the present setup has been further analyzed by the authors in (Famiglietti and Lecuona, 2021b). In that study, either static and dynamic receiver numerical models of the solar field and receiver tube are validated against experimental data from transient heating and cooling tests devised for this purpose. Linear Fresnel collector operation is there analyzed, obtaining an experimental estimation of the optical efficiency. In addition, experimental correction factors for the optical efficiency are proposed for improving the accuracy of the optical performance prediction of the specific LFC employed, although the methodology implemented holds general validity.

Regarding the turbocharger behavior and the pumping power consumption in the present setup, some considerations can be formulated from the experiments overview. According to the original T-SAH concept, the turbocharger increased the air pressure into the T-SAH tubes, recovering compressing power through the turbine. The auxiliary compressor is supposed to be needed only for the starting transient and bypassed once steady-state condition would be reached. Moreover, in the above experiment, it was needed to sustain the turbocharger freewheeling under the operating steady-state conditions tested. The too small turbocharger limits compressor and turbine efficiencies, which in this case have modest values owing to the small size. In addition, due to the relatively small scale of the solar field, the turbocharger does not operate under optimal conditions, being large in size for the mass flow employed.

Nevertheless, the beneficial effect of turbocharging on auxiliary pumping power reduction can be deduced by observing Fig.4. As the turbocharger speed and pressure ratio increase, the overpressure $p_{1t} - p_{0t}$ imposed by the auxiliary compressor decreases slightly. In a T-SAH with higher performances, expected when scaling up to industrial sizes, $p_{1t} = p_{0t}$ would be reached in steady-state conditions, as numerically demonstrated by (Famiglietti *et al.*, 2021).

Within the limited performances of the present experimental setup, a more significant auxiliary over-pressure reduction trend is observed in the second test presented as follows. There, higher inlet turbine temperatures are obtained with the aid of an electrical post-heating unit, Fig.1. The three Fresnel modules were in tracking mode throughout the experiment. The auxiliary compressor was active. The experimental post-heating unit was activated during the experiment with increasing electrical power, delivering an additional thermal power to air $\dot{Q}_{ph}$. The use of an electrical post-heating unit downstream the solar tube allowed achieving a higher turbine inlet enthalpy, in this case by increasing temperature, without the risk of receiver tube overheating, hence extending the turbocharger testing range without a larger solar facility neither a smaller turbocharger, which would be even less efficient.

The use of electrical post-heating is only for experimental purposes, extending the turbocharger testing range, and would not be implemented in a real industrial plant, being not convenient to dissipate electricity into heat. Fig.5 reports results. An inlet turbine temperature T_3 =570 °C is reached, while the receiver outlet temperature remains at 430 °C as maximum, Fig.5(a). The increased turbine power brings the turbocharger to higher speed and a better operating condition, pumping slightly greater air mass flow rate, Fig.5(b). Despite this, the pressure drop across the receiver tubes drops thanks to the effect of increased pressure, which goes up to 1.6 bar, Fig. 5(c). As mentioned, the reduction of auxiliary overpressure $p_{1t} - p_{0t}$ required decrease with turbocharger speed and inlet turbine temperature, and it is more significant than in the previous case.

A deep analysis of turbocharger performance in the present setup is presented by the authors in (Famiglietti and Lecuona, 2021a). It includes both the adiabatic and diabatic behaviors of the turbocharger under the operating conditions achieved within the proposed T-SAH layout. Experimental 'hot' test performances obtained have been contrasted with the 'cold' performances predicted using extrapolation of the manufacturer's maps, allowing to quantify the parasitic heat transfer phenomena according to a simplified modeling. The analysis shows how the small turbocharger used is affected by thermal losses to ambient and to lubrication oil which downgrades its performance. Such diabatic behavior is expected to be negligible in well-insulated, ball bearings, larger size turbochargers which would be used in industrial-scale plants, as those simulated in (Famiglietti *et al.*, 2021). They further discuss the auxiliary compressor behavior and underpins the critical aspect for scaling up the technology.

Globally, the experimental results reported in the present study show the behavior of a small-scale T-SAH allowing its characterization under real ambient conditions, underpinning critical aspects and possible improvements. The experimental data acquired allows the numerical model validation and tuning, preparing the scaling-up studies carried out in the following.

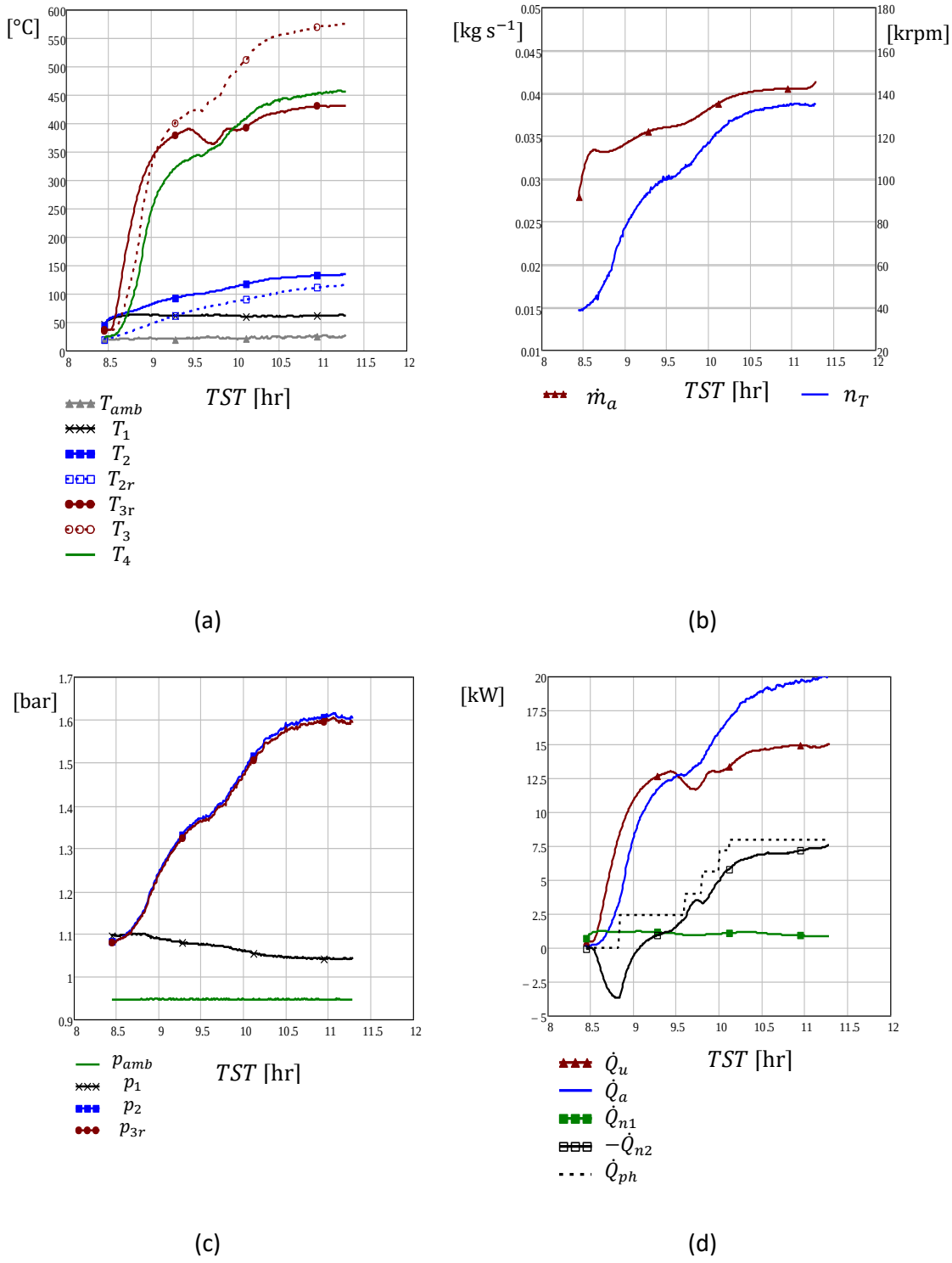

Fig. 5. Experimental results, T-SAH operation along a sunny summer day, experimental post-heating unit ON, vs. true solar time. (a) Temperatures. (b) Mass flow rate and speed. (c) Pressures. (d) Thermal powers.

4. Conclusions

The analysis of collected data sets allows scrutinizing several aspects of the installation and original concept of T-SAH. The results indicate the feasibility of direct solar air heating inside standard evacuated tubes up to

500 °C. Low internal heat transfer, established according to air thermal properties and mass flow rate, combined with the inhomogeneous circumferential distribution of concentrated heat flux, induce tube bending which can cause glass cover contact, if excessive. Receiver tube bending is noticed during the experiments at high temperatures as well as during transient heating. Nevertheless, no damage to the receiver has been detected.
Outlet turbine temperatures between 300 and 400°C have been reached, according to the purpose of the technology and theoretical predictions. The behavior of the turbocharger and auxiliary blower has been investigated. The small-scale facility did not allow to reach optimum operating conditions in the implementation here considered, due to low turbocharger efficiency, typical of small size turbochargers. Nevertheless, the analysis carried out indicates the relevant features of the system when scaled up to typical sizes.

5. References

Archimede Solar Energy (accessed May 2018). Available at: http://www.archimedesolarenergy.it/.

Famiglietti, A. et al. (2020) 'Direct solar production of medium temperature hot air for industrial applications in linear concentrating solar collectors using an open Brayton cycle . Viability analysis', 169(September 2019). Available at: https://doi.org/10.1016/j.applthermaleng.2020.114914.

Famiglietti, A. et al. (2021) 'Turbo-assisted direct solar air heater for medium temperature industrial processes using Linear Fresnel Collectors . Assessment on daily and yearly basis', 223. Available at: https://doi.org/10.1016/j.energy.2021.120011.

Famiglietti, A. and Lecuona, A. (2021a) 'Direct solar air heating inside small-scale linear Fresnel collector assisted by a turbocharger : Experimental characterization', Applied Thermal Engineering, 196(September). doi: 10.1016/j.applthermaleng.2021.117323.

Famiglietti, A. and Lecuona, A. (2021b) 'Small-scale linear Fresnel collector using air as heat transfer fl uid : Experimental characterization', 176.

Farjana, S. H. et al. (2018) 'Solar process heat in industrial systems – A global review', Renewable and Sustainable Energy Reviews, 82(August 2017), pp. 2270–2286. doi: 10.1016/j.rser.2017.08.065.

Garrett Advancing Motion (accessed June 2019). Available at: https://www.garrettmotion.com/.

Rehman, S. et al. (2019) 'Experimental evaluation of solar thermal performance of linear Fresnel reflector', Journal of Mechanical Science and Technology, 33(9), pp. 4555–4562. doi: 10.1007/s12206-019-0852-6.

SHIP Database (accessed January 2020). Available at: http://ship-plants.info/.

Solatom (accessed January 2020) SOLAR STEAM FOR INDUSTRIAL PROCESSES. Available at: http://www.solatom.com/.

Zahler, C. and Iglauer, O. (2012) 'Solar process heat for sustainable automobile manufacturing', Energy Procedia, 30, pp. 775–782. doi: 10.1016/j.egypro.2012.11.088.